Available online at www.sciencedirect.com
ScienceDirect
Composites Science and Technology 68 (2008) 1671–1678
COMPOSITES SCIENCE AND TECHNOLOGY
www.elsevier.com/locate/compscitech

Mechanics of textile composites: Micro-geometry

Yuyang Miao [a], Eric Zhou [a], Youqi Wang [a,*], Bryan A. Cheeseman [b]

[a] Department of Mechanical and Nuclear Engineering, Kansas State University, Manhattan, KS 66506, USA
[b] US Army Research Laboratory, Aberdeen Proving Ground, MD 21005, USA

Received 5 July 2007; received in revised form 18 November 2007; accepted 7 February 2008
Available online 23 February 2008

Abstract

Textile fabric geometry determines textile composite properties. Textile process mechanics determines fabric geometry. In previous papers, the authors proposed a digital element model to generate textile composite geometry by simulating the textile process. The greatest difficulty encountered with its employment in engineering practice is efficiency. A full scale fiber-based digital element analysis would consume huge computational resources. Two advances are developed in this paper to overcome the problem of efficiency. An improved contact-element formulation is developed first. The new formulation improves accuracy. As such, it permits a coarse digital element mesh. Then, a static relaxation algorithm to determine fabric micro-geometry is established to replace step-by-step textile process simulation. Employing the modified contact element formulation in the static relaxation approach, the required computer resource is only 1–2% of the resource required by the original process. Two critical issues with regards to the digital element mesh are also examined: yarn discretization and initial yarn cross-section shape. Fabric geometries derived from digital element analysis are compared to experimental results.

Keywords: A. Textile composites; A. Fabrics/textiles; C. Finite element analysis (FEA); B. Modelling; Fabric geometry

1. Introduction

Textile fabric geometry determines textile composite properties. Textile process mechanics determines fabric geometry. Therefore, textile composite mechanics includes two important aspects: (1) to determine fabric geometry based upon textile process mechanics and (2) to determine textile composite properties based upon fabric geometry. This paper deals with the determination of textile fabric micro-geometry.

Textile fabric micro-geometry is determined by (1) textile process kinematics and (2) forces applied to yarns/fibers during the textile forming process. Process kinematics determines basic internal yarn structural patterns of fabrics, called fabric topology. Forces applied to yarns/fibers during the textile forming process determine detailed micro-geometry, such as yarn cross-section shapes, individual fiber paths within a yarn and yarn curvatures.

Wang and Sun [1–4] developed a digital element approach to simulate the textile process. Using the digital element approach, the textile process was modelled as a quasi-static structural mechanics problem with boundary conditions. Detailed fabric geometry was generated with both yarn level and fiber-level micro-structures observed. At the yarn level, both yarn paths and cross-section shapes were defined; at the fiber-level, fiber orientations and fiber volume fractions were determined point-by-point.

The greatest difficulty encountered for the application of the digital element approach in engineering practice is the efficiency of the numerical model. A full scale fiber-based digital element analysis would consume huge computational resources. Two advances are developed in this paper to overcome the efficiency problem. Firstly, an improved contact-element formulation is developed. The new formulation improves accuracy. This permits a coarser digital element mesh. Only 1/4 amount of elements are required to

* Corresponding author. Tel.: +1 785 532 7181; fax: +785 532 7057.
E-mail address: wang@mne.ksu.edu (Y. Wang).

0266-3538/$ - see front matter © 2008 Elsevier Ltd. All rights reserved.
doi:10.1016/j.compscitech.2008.02.018

simulate the same textile process with the same accuracy. This saves 90% of computation time. Secondly, a static relaxation algorithm to determine fabric micro-geometry is established to replace step-by-step textile process simulation. This further reduces computation time by 80–90%. Employing the modified contact element formulation in the static relaxation approach, the required computation time is only 1–2% of the computation time required by the original process. This makes the digital element a practical computational tool for the determination of textile fabric micro-geometry.

In addition, the accuracy and convergence of the digital element method are explicated. Two critical issues with regards to the digital element mesh receive close examination: yarn discretization and initial yarn cross-section shape. Fabric geometries derived from various digital element meshes are compared to each other and to experimental results.

The paper is constructed in the following order: (1) detailed description of the original digital element formulation, (2) modified contact element formulation, (3) accuracy analysis, (4) static relaxation algorithm, (5) fabric micro-geometries and comparison between numerical results and microscopic pictures.

2. Digital element approach

2.1. Concept of original digital element approach

The digital element approach is the first analytical procedure that models textile process and fabric deformation based upon inherent textile physics, such as yarn-to-yarn and fiber-to-fiber interactions.

Fig. 1 illustrates three key concepts in the approach: digital-chain, yarn assembly and contact between digital chains. Refer to Fig. 1a. A digital chain is a physical representation of a fiber. It consists of many small-digital-rod-elements. These small digital elements are connected by frictionless pins along the axial axis. The digital chain is fully flexible and can deform freely, as shown in Fig. 1b. Digital chains are organized into bundles, forming a yarn. The yarn cross-section shape deforms under external load. Fig. 1b shows a deformed yarn.

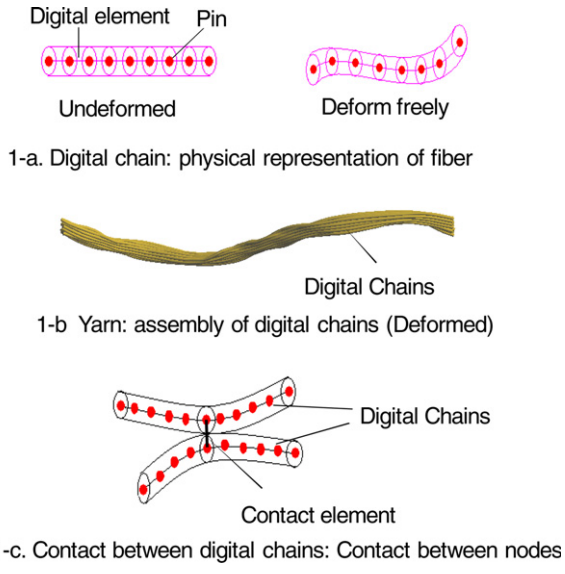

Fig. 1. Concept of digital element approach.

Contact among digital chains is modelled by contact elements. If the distance between two nodes located on two neighbouring digital chains is smaller than the chain diameter, a contact element is inserted between these two nodes, as shown in Fig. 1c. The contact element can support both compressive and friction force. In each loading step, a new contact element is established if two digital chains move to contact each other. Upon separation of two contacting digital chains, the exiting contact element is removed.

A textile process can be simulated as a quasi-static problem. Boundary conditions are defined based upon the process and a fabric is generated step by step.

2.2. Element stiffness matrices

2.2.1. Digital element

Digital-rod-elements are connected by pins. Each element has two end nodes: node i and node j. If the chain is fully flexible, the stiffness matrix of the digital element should be the same as the stiffness matrix of 3-D truss element. However, the global stiffness matrix is often singular if the truss element stiffness matrix is used. The numerical process is instable. In order to prevent global stiffness matrix singularity, a small transverse stiffness is introduced. The element stiffness is expressed as

$$[\mathbf{K}]^e = \frac{EA}{L_\mathrm{d}} \begin{bmatrix} 1 & 0 & 0 & -1 & 0 & 0 \\ 0 & \Delta & 0 & 0 & -\Delta & 0 \\ 0 & 0 & \Delta & 0 & 0 & -\Delta \\ -1 & 0 & 0 & 1 & 0 & 0 \\ 0 & -\Delta & 0 & 0 & \Delta & 0 \\ 0 & 0 & -\Delta & 0 & 0 & \Delta \end{bmatrix} \tag{1}$$

where E is fiber modulus, L_d is digital element length and A is element cross-section area. Δ defines transverse stiffness, which is a small number. In numerical simulation, a number between 10^{-5} and 10^{-6} is adopted. Physically, it is equivalent to a small torsional spring located at the midpoint between two end nodes.

2.2.2. Contact element

Contact between two digital chains is represented by contact between two nodes. If distance between two nodes from two neighbouring chains is smaller than chain diameter, a contact element is built between them. The contact element used in this simulation is identical to the 3-D point-to-point contact element used in ANSYS [5].

If contact occurs between two nodes, one of two kinds of physical conditions would exist: sticking or sliding.

2.2.2.1. Stick contact. Two chains will stick together if $\mu \mathbf{F}_n > |\mathbf{F}_s|$, where μ is friction coefficient, $\mathbf{F}_n$ is compressive force between two nodes, and $\mathbf{F}_s$ is shear force between two nodes. The stiffness matrix of the contact element can be expressed as [5]

$$\begin{bmatrix} k_n & 0 & 0 & -k_n & 0 & 0 \\ 0 & -k_s & 0 & 0 & +k_s & 0 \\ 0 & 0 & -k_s & 0 & 0 & +k_s \\ -k_n & 0 & 0 & k_n & 0 & 0 \\ 0 & +k_s & 0 & 0 & -k_s & 0 \\ 0 & 0 & +k_s & 0 & 0 & -k_s \end{bmatrix} \quad (2)$$

where k_n and k_s are compressive stiffness coefficient and lateral stiffness coefficient, respectively.

It is difficult to determine exact compressive stiffness and lateral stiffness. Compressive stiffness depends upon fiber transverse modulus, which is almost completely unavailable in fiber data sheets. Only limited data can be found in the literature. However, minimal fiber cross-section deformation occurs during the textile process. Fiber-to-fiber contact can be modelled as either rigid or elastic. Numerical results show that both models provide almost identical fabric micro-geometry. Therefore, rather than using an exact compressive stiffness for each contact element, one can simply choose a k_n in the same magnitude of order as the digital element longitudinal stiffness.

The lateral stiffness coefficient k_s is assumed to be

$$k_s = \mu k_n \quad (3)$$

2.2.2.2. Sliding contact. Sliding occurs when $\mu \mathbf{F}_n <= |\mathbf{F}_s|$. When sliding occurs, lateral stiffness becomes zero. Contact element stiffness matrix can thus be written as [5]

$$\begin{bmatrix} k_n & 0 & 0 & -k_n & 0 & 0 \\ 0 & 0 & 0 & 0 & 0 & 0 \\ 0 & 0 & 0 & 0 & 0 & 0 \\ -k_n & 0 & 0 & k_n & 0 & 0 \\ 0 & 0 & 0 & 0 & 0 & 0 \\ 0 & 0 & 0 & 0 & 0 & 0 \end{bmatrix} \quad (4)$$

2.2.3. Residual nodal force

Residual nodal force is the sum of internal and external nodal forces. External nodal force is pre-defined; internal nodal force must be calculated in each simulation step.

Refer to Fig. 2a. Elements k and l are two neighbouring digital elements belonging to the same chain. They are connected by node i. Further, node i also contacts node j, which is located on the other digital chain. A contact element m is inserted between i and j. Internal nodal forces applied to node i are induced by (1) digital element tension and (2) contact force between two digital chains. Referring to Fig. 2b, four nodal forces are applied to node i: $\mathbf{F}_i^{(k)}$ and $\mathbf{F}_i^{(l)}$ are induced by element tension; $\mathbf{F}_{in}^{(m)}$ and $\mathbf{F}_{is}^{(m)}$ are induced by chain-to-chain compression and friction, respectively.

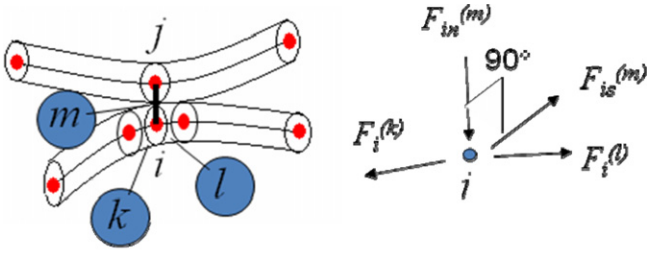

(a) Neighbouring elements (b) Force applied to node i

Fig. 2. Forces applied to a node.

The magnitudes of $\mathbf{F}_i^{(k)}$ and $\mathbf{F}_i^{(l)}$ are equal to the tensions of element k and element l, respectively. They can be derived as

$$\mathbf{F}_i^{(k)} = \epsilon^{(k)} EA, \quad \mathbf{F}_i^{(l)} = \epsilon^{(l)} EA \quad (5)$$

where $\varepsilon^{(k)}$ and $\varepsilon^{(l)}$ denote element strain, E denotes fiber modulus and A denotes element cross-section area. Force direction is aligned with axial direction.

Contact compressive force increment $\Delta \mathbf{F}_{in}^{(m)}$ between nodes i and j can be calculated as

$$\Delta \mathbf{F}_{in}^{(m)} = k_n \Delta L_c \quad (6)$$

where L_c is contact element length, which represents the distance between two digital chains.

For the stick state, friction increment $\Delta \mathbf{F}_{is}^{(m)}$ during each loading step is derived using the following equation:

$$\Delta \mathbf{F}_{is}^{(m)} = k_s \Delta u_s^{i-j} \quad (7\text{-a})$$

where is relative lateral displacement between nodes i and j during the loading step. For the sliding state, total friction force is derived using the following equation:

$$\mathbf{F}_{is}^{(m)} = \mu \mathbf{F}_{in}^{(m)} \quad (7\text{-b})$$

The direction of friction force is always in the opposite direction of the relative lateral displacement.

2.2.4. Numerical procedures

A textile process is modelled as a quasi-static process. After all element stiffness matrices are generated, they are transformed into global coordinates. The global stiffness matrix is assembled in a manner analogous to conventional finite element analysis. A textile process can thus be simulated step-by-step. The problem is non-linear because large displacements occur during the textile process. During numerical simulation, orientations of all elements must be calculated in each step and element stiffness matrices must be transformed into global coordinates. The global stiffness matrix must then be reassembled accordingly.

3. Modified contact element

3.1. Existing problems

In the original model, the contact of digital chains is modelled by contact of nodes. Contact element length

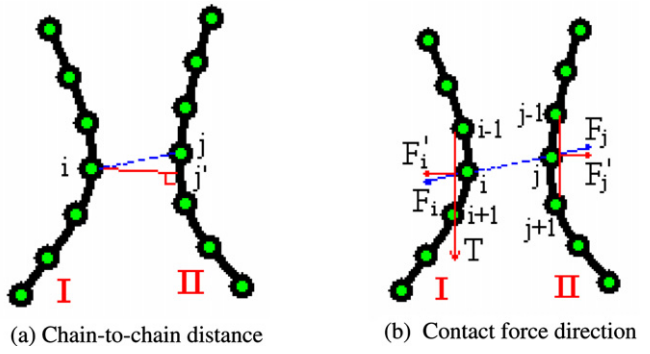

(a) Chain-to-chain distance (b) Contact force direction

Fig. 3. Contact element modification.

represents distance between two digital chains. The axial direction of the contact element is assumed to align with the compressive force direction between them. This is true only if the digital-rod-element length approaches zero. As such, a fine resolution in digital element analysis is critical for solution accuracy. Refer to Fig. 3. If a coarse mesh, i.e. a longer digital element length, is adopted, contact element length would no longer equal distance between two digital chains and calculated compressive force would not be perpendicular to two contacting digital chains. Both the magnitude and the direction of compressive forces between two digital chains could not be calculated accurately. The lateral component of this calculated compressive force acts as "artificial friction". It prevents relative sliding motion between digital chains even when the friction coefficient is assumed to be zero. In order to avoid the "artificial friction", a digital element length of 1/4 element diameter or less is recommended.

3.2. Modification of the contact element

Two modifications are introduced to correct the aforementioned problems. The first relates to calculation of contact distance between two digital chains. The distance, i.e., the contact element length, is calculated based upon node-to-element distance rather than node-no-node distance, as is done in the original model. Refer to Fig. 3a. Distance between points i and j', rather than distance between nodes i and j, is used to calculate the magnitude of compressive contact force applied to nodes i.

The second modification relates to direction of compressive contact force between two digital chains. It is assumed that compressive contact force is perpendicular to digital chain I at node i, which is in direction from point j' to node i. Refer to Fig. 3b. Compressive force direction at node i is defined by force $\mathbf{F}_i'$, which is perpendicular to the tangential vector $\mathbf{T}$. Therefore, the compressive force applied to node i can be derived as

$$\mathbf{F}_i' = \frac{\mathbf{T}}{|\mathbf{T}|} \times \frac{\mathbf{F}_i \times \mathbf{T}}{|\mathbf{F}_i \times \mathbf{T}|} |\mathbf{F}_i| \tag{8}$$

where $|\mathbf{F}_i|$ is calculated based upon the modified distance, i.e., the distance between node i and point j', as shown in Fig. 3a. Similarly, $\mathbf{F}_j'$ can be derived.

It is found that these modifications remove "artificial friction". The modified contact element allows employment of a relatively coarse digital element mesh. With the modified contact element formulation, we recommend adoption of an element-length/diameter ratio of 0.75-1.25. Compared to the original formulation, only 1/4 of elements are required to simulate a textile process with a similar or better accuracy. This means only 10% computer resource is required to solve the same problem.

4. Accuracy analysis

In a finite element analysis, accuracy of the numerical result depends upon size of the element. In digital element analysis, accuracy of the numerical result depends upon the digital element mesh. The digital element mesh includes two aspects: element length and yarn representation. It has been found that numerical results become stable if digital element length is smaller than element diameter. In this section, yarn representation is discussed.

Yarn representation includes two aspects. One is the number of digital chains that represent a yarn. The other is the initial chain arrangement inside yarns. Both are examined in the subsequent two sub-sections.

4.1. Yarn discretization

A yarn is modelled as an assembly of digital chains. Textile yarns commonly consist of thousands or ten-thousands of fibers. In numerical analysis, it is found that yarn cross-section shape can be represented by a far smaller number of digital chains. For example, an almost identical micro-geometry is derived from the following two yarn models: one yarn consists of 100 digital chains, the other 50 digital chains. As such, a question is raised: how many digital chains are necessary and sufficient to represent a yarn in digital element analysis in order to achieve an acceptably accurate geometric shape? In order to answer this question, yarn models with different numbers of digital chains are used in 2-D woven and 3-D braiding processes. The derived micro-geometries are compared and reviewed. Two types of fabrics are employed in this assessment: 2-D woven and 3-D braided fabrics.

4.1.1. 2-D woven fabrics

Firstly, a 2-D woven fabric is created by digital element simulations. Yarns, modelled as 19, 37, 52 and 69 digital chains, are employed. Fig. 4 shows a comparison between an actual fabric cross-section and cross-sections derived using 19, 37, 52 and 69 digital-chain yarns. It appears that fabric cross-section geometries derived using the 69 and 52 digital-chain yarn models match the actual cross-section shape a litter bit better than do the other two cross-section shapes derived using 19 and 37 digital-chain yarn models.

4.1.2. 3-D braided fabrics

In this subsection, two 3-D braided fabric micro-geometries are compared. One fabric is generated by a 19 digital

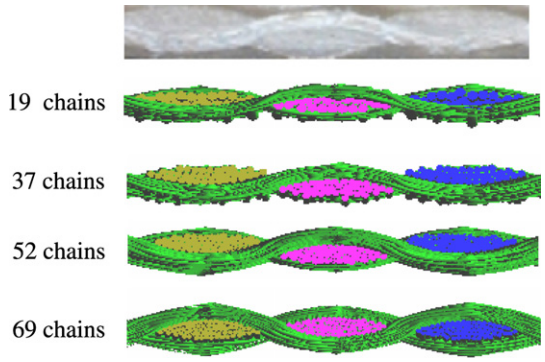

Fig. 4. Comparison between numerical results and experimental observation.

yarn model, the other by a 37 digital-chain yarn model. Their micro-geometries are compared in Fig. 5. The left picture is a fabric created by the 19 digital-chain yarn model. Three yarns are taken from the fabric. The picture in the middle is a fabric created by the 37 digital-chain yarn model. Three corresponding yarns are taken from the fabric. On the right side, images of yarns composed of 19 digital chains are superimposed on images of yarns composed of 37 digital chains. They overlap.

Cross-section shapes of these two braided fabrics are shown in Fig. 6. Cross-section shapes of five positions, C1, C2, C3, C4 and C5, are compared. Five cross-section shapes in the first row are taken from fabric generated by the 19 digital-chain yarn model. The second row shows cross-section shapes taken from fabric generated by the 37 digital-chain yarn model. The third row shows the comparison. Cross-section images of fabric created by the 19 digital-chain yarn model are superimposed over cross-section images of fabric created by the 37 digital-chain yarn model. Again, similar micro-geometries of cross-section shapes are seen. It appears the 19 digital-chain yarn model is sufficient in numerical simulation to predict 3-D braided fabric micro-geometries.

4.2. Yarn initial shape

In all aforementioned examples, a circular initial shape is employed in digital simulations. In reality, yarns have irregular cross-section shapes along their axial paths prior to a textile process. However, it is common to see a consistent micro-geometry repetition of yarn cross-section shapes inside a textile composite. For example, Fig. 7 shows a cross-section of 3-D braided composites. Initial irregular yarn cross-section shapes appear to have no significant impact on final yarn micro-geometry. If this is true, various initial shapes could be adopted in numerical simulations. In order to verify this issue, both circular and rectangular yarn cross-sections are used to generate a 2-D woven fabric. Two initial digital-chain positions for these two yarn cross-sections are shown in Fig. 8. Each yarn consists of 19 digital chains. Derived warp and weft yarn paths are also shown in Fig. 8. Similarly, warp and weft yarn cross-sections are compared. It is found that both yarn paths and yarn cross-section shapes derived from these two examples almost completely overlap each other.

Same conclusions are found from comparison of 3-D braided fabrics generated using these two initial yarn shapes. Therefore, one concludes that an assumed initial yarn shape has minimal influence on final fabric micro-geometry generated by use of digital element analysis. Various initial yarn cross-section geometries can thus be adopted in numerical simulation.

5. Static relaxation approach

The digital element approach has been successfully used to simulate 2-D weaving and 3-D braiding processes. However, simulation of the textile process step-by-step is too time-consuming. In order to solve this problem, a static relaxation approach is developed. This model assumes fabric micro-geometries are primarily determined (1) by fabric topology and (2) by the final state of yarn tensions and

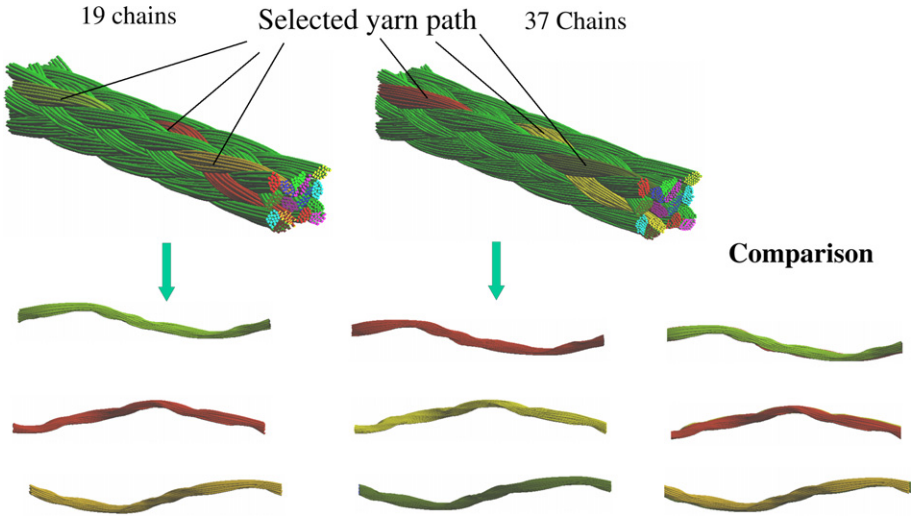

Fig. 5. Yarn geometry of 3-D braided fabric.

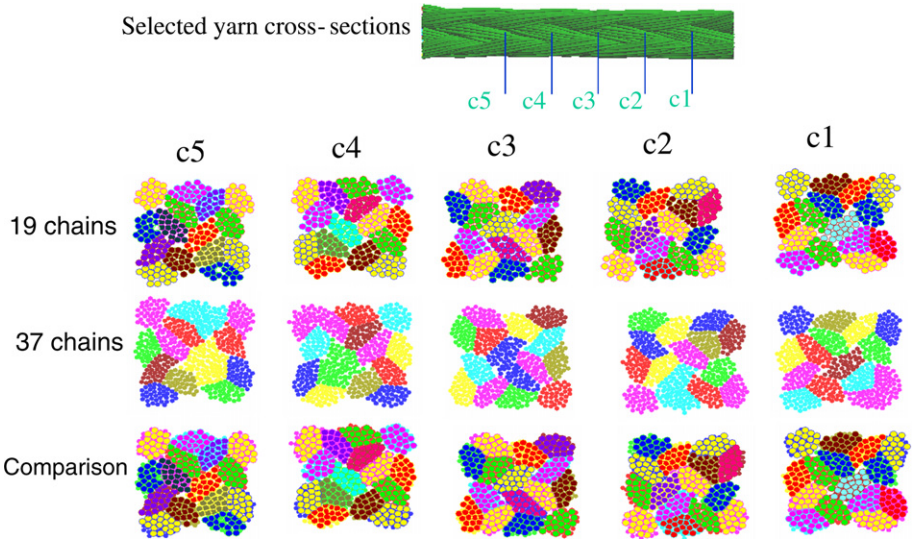

Fig. 6. Micro-geometries of 3-D braided fabric cross-sections.

Fig. 7. Consistent micro-geometry repetition of 3-D braiding composite cross-section.

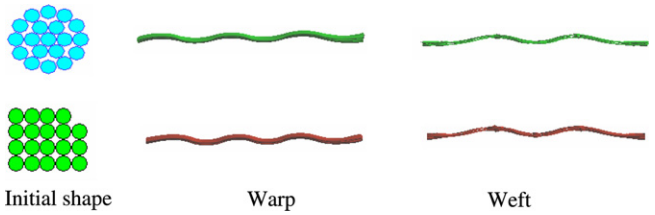

Fig. 8. Yarn path comparisons.

yarn-to-yarn compressions. The effects of yarn-to-yarn friction and chain-to-chain friction on micro-geometries are neglected.

The static relaxation approach generally includes three steps. In the first step, an initial guess fabric structure is established based upon fabric topology. In the second step, each yarn is discretized into 19–25 digital chains and initial chain strain is applied to each digital chain. In the third step, non-equilibrium force applied to each node is calculated and then relaxed. The example of 3-D braided fabric generation is used as an example to explain the process. The geometry of the 3-D braided fabric is compared to the microscopic picture. The comparison indicates that the static relaxation approach is a valid way to generate textile fabric micro-geometry. Two types of 3-D woven fabrics are created using this method.

Compared to step-by-step textile simulation, less than 10% computer resource is required to generate the same fabric.

5.1. 3-D braided fabrics

A 13 × 5 3-D braided fabric is generated using the static relaxation approach. The numerical procedure can be divided into three steps, as shown in Fig. 9.

Step 1: Determine a guess structure based upon fabric topology. The guess structure has the same basic yarn structural pattern as the actual fabric. It is determined by process kinematics. In this example, the guess structure is derived from the simulation of a step-by-step 3-D braiding process using a single digital-chain yarn model. It is shown in Fig. 9a. Because the yarn is composed of only one digital chain, yarn cross-sections are all circular. The numerical simulation does not provide a detailed micro-geometry, including yarn cross-section shape and yarn/fiber spatial paths. This is determined by a force relaxation approach as seem in step 2 and step 3.

Step 2: Yarn discretization. In step 2, each yarn is discretized into 19 digital chains, as shown in Fig. 9b.

Step 3: Static relaxation. In the actual textile process, tension is applied to yarns and fibers, creating a tight fabric structure. In order to imitate the tension effect, a pre-tensile-strain (or stress) is assumed for each digital chain of the guess structure. Non-equilibrium pre-nodal-forces are thus produced. The fabric deforms until reaching a new equilibrium state. In numerical analysis, the pre-tensile-strain is applied incrementally. Each loading step includes the following sub-steps:

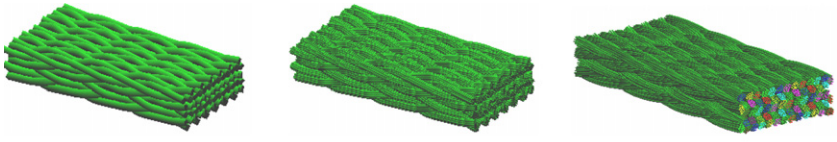

(a) Initial fabric geometry (b) Yarn Discretization (c) Relaxed micro-geometry

Fig. 9. Relaxation procedure for a 3-D braided fabric.

1. Assume an increment pre-tensile strain.
2. Calculate nodal forces.
3. Assemble global stiffness matrix.
4. Solve nodal displacement from equation:

$$[\mathbf{K}]\{U\} = \{\mathbf{F}\} \tag{9}$$

5. Calculate new nodal positions:

$$\{X\} = \{X\} + \{U\} \tag{10}$$

6. Return to sub-step 2 until nodal force is smaller than an allowable error.
7. Calculate digital chain and yarn tensions.

The numerical simulation continues until a targeted yarn tension is achieved.

Fig. 9c shows the derived micro-geometry of the 3-D braided fabric. Two representative cross-sections of the derived fabric are compared to cross-sections of an actual 3-D braided fabric in Figs. 10a and b. One can see the similarity of the cross-section geometries derived from the static relaxation process and from the actual fabric. It validates the approach.

5.2. 3-D woven fabrics

Digital element analysis can also be used to generate other 3-D fabrics. Fig. 11 shows two types of 3-D woven fabrics: a layer-to-layer 3-D interlock woven fabric and a through-the-thickness 3-D interlock woven fabric.

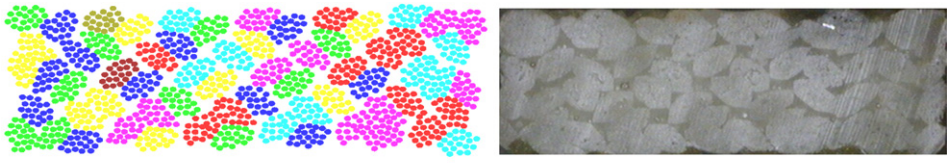

(a) Cross-section 1

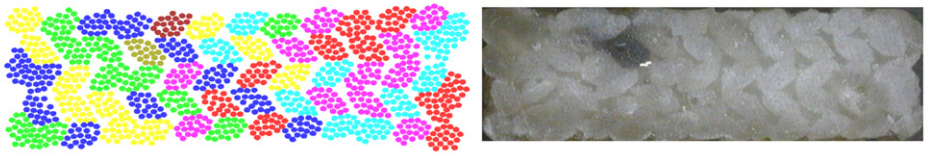

(b) Cross-section 2

Fig. 10. Comparison of cross-sections.

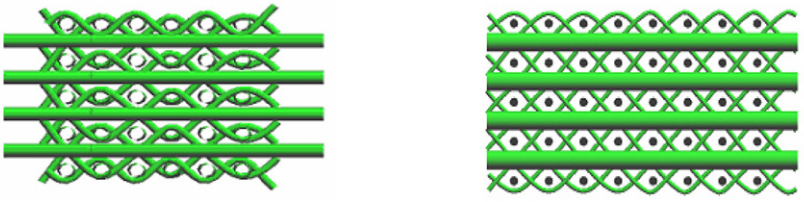

Layer-to-layer Through-the-thickness angle interlock

(a) Initial fabric geometry

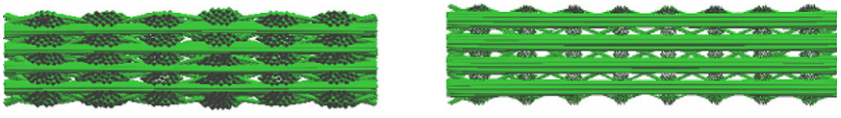

Layer-to-layer Through-the-thickness angle interlock

(b) Relaxed micro-geometry

Fig. 11. Relaxation processes of 3-D woven fabrics.

Fig. 11a shows the basic yarn structural patterns for these two fabrics, which are available from the literature [6]. They are used as initial guess fabrics. Final micro-geometries derived from the static relaxation approach are shown in Fig. 11b. The geometrical models for these two 3-D woven fabrics have been used to predict the mechanical properties of composites made from these two fabrics [7].

6. Conclusions

Conclusions reached from the research presented in this paper are:

A modified contact element formulation is proposed for digital element analysis. The new contact element improves the accuracy of contact forces. For this reason, a coarser digital element mesh is permitted. This saves 90% of computing time.

With the improved digital element analysis, 2-D weaving and 3-D braiding processes are simulated. 19, 37, 52 and 67 digital-chain yarn models are used for the simulation of the 2-D weaving process; 19 and 37 digital-chain yarn models are used for the simulation of the 3-D braiding process. Generated fabric geometries are compared to each other and to experimental observation. Among the four 2-D woven fabrics, it appears that (a) yarn paths are almost identical and (b) fabric cross-section geometries derived using the 69 and 52 digital-chain yarn models match the actual cross-section shape a little better than do the other two cross-section shapes derived using 19 and 37 digital-chain yarn models. Micro-geometries of the two braided fabrics are also compared with each other. The corresponding yarn shapes from the two fabrics are almost identical. It seems that the 19 digital-chain yarn model has sufficient accuracy to predict micro-geometries of 3-D braided fabrics.

Two 2-D woven fabrics, one generated using an initial yarn with a circular cross-section and the other generated using an initial yarn with a square cross-section, have similar micro-geometries. Initial yarn cross-section shapes do not alter numerical results in a significant matter. Therefore, different initial cross-section shapes can be selected in numerical simulations.

A static relaxation approach is proposed for the determination of fabric micro-geometry. This process uses less than 10% computer resources compared to a step-by-step textile process simulation using a multi-digital-chain yarn model. Employing the modified contact element formulation within a static relaxation process, the required computing time is only 1-2% of computing time required by the original process. A 3-D braided fabric and two types of 3-D woven fabrics are generated using the static relaxation approach. The micro-geometry of the 3-D braided fabrics generated by numerical simulation is compared to experimental results. The comparison validates the static relaxation approach.

Acknowledgement

The financial support provided by the U.S. Army Research Laboratory is acknowledged.

References

[1] Wang YQ, Sun XK. Determining the geometry of textile preforms using finite element analysis. In: 9th Annual technical conference of American society for composites; 2000. p. 485–92.
[2] Sun XK, Wang YQ. Geometry of 3-D braiding rectangular preform with axial yarns. In: 46th International SAMPE symposium, Long Beach, CA; 2001. p. 245–53.
[3] Wang YQ, Sun XK. Digital element simulation of textile processes. Compos Sci Technol 2001;63:311–9.
[4] Zhou G, Sun XK, Wang YQ. Multi-chain digital element analysis in textile mechanics. Compos Sci Technol 2004;64:239–44.
[5] ANSYS Element Manual, Contact element 52: 3-D point-to-point contact element.
[6] Cox BN, Carter WC, Fleck NA. A binary model of textile composite – I. Formulation. Acta Metal Mater 1994;42(10):3463–79.
[7] Miao YY. Mechanics of textile composites: from micro-geometry to mechanical properties, PhD Dissertation, Kansas State University; 2005.